Quantal Brownian motion in stationary and nonstationary fermionic reservoirs

E. S. Hernández and C. O. Dorso
Departamento de Física, Facultad de Ciencias Exactas y Naturales, Universidad de Buenos Aires, 1428 Buenos Aires, Aires, Argentina
(Received 1 November 1982)

A model for collective mode damping in nuclei is devised in the frame of a theory of irreversible evolution. The decay width of a fast nuclear vibration, originated in its coupling to the remaining nuclear degrees of freedom, is calculated in a dynamical fashion. To this aim, a set of equations is proposed that describes the simultaneous dynamics of the oscillation or its associated array of bosons and of the interacting fermions that play the role of a heat reservoir. These are, respectively, a quantal master equation and modified kinetic one. The two of them exhibit their mutual coupling in the non-Hermitian terms of their generators of motion. The equations are worked out in detail in (a) the weak-coupling approximation plus (b) the very-close-to-equilibration regime plus (c) the energy-conserving description of intermediate processes. With hypothesis (c) the heat bath can be regarded as lying in a steady state at all times and the master equation is solved for different temperatures and phonon energies. The damping width of the oscillations is thus quantitatively predicted.

[NUCLEAR STRUCTURE Damping width. High-frequency collective modes. Nonstationary fermionic heat reservoir. Coupled dynamics. Quantal master equation. Modified BBGKY hierarchy. Modified kinetic equation. Single-particle lifetime. Temperature-dependent transition rates. Thermal equilibration. Irreversible evolution with effective collision frequency or relaxation time.]

I. INTRODUCTION

High-energy nuclear vibrations constitute beautiful examples of damped macroscopic motion in finite systems. Since the observation of the giant dipole resonance, that gave a strong motivation to the particle-hole model of collective oscillations,[1,2] a wealth of literature has dealt with the experimental recording, the theoretical frame, and the overall systematics of these modes,[3–11] whose domain has enlarged with the observation of higher resonant multipolarities.[9]

Among the various interesting features of high-frequency vibrations, their observed widths have been regarded as manifestations of dissipative coupling to some other macroscopic or particle coordinates associated to the nucleus. The viewpoints adopted to describe the resonance broadenings range from the assignment of particle-hole (p-h) widths[12–17] to the construction of complex dispersion relations for the multipole density oscillations in a spherical cavity[3,18–21] in the frame of the nuclear hydrodynamic model. Different versions of the same problem could be quoted, in particular the elastic-vibration description,[22] the one-body dissipation model,[23] and Green's functions method in the spirit of perturbation theory.[12–17,24] These theories and models, like their counterparts, namely those aiming at the reproduction of the peak resonant energy, focus upon very specific features of nuclear dynamics, like the real and imaginary part of an energy eigenvalue in a dispersion law for high-frequency collective motion. It is our purpose to provide a frame in which both the macroscopic and the intrinsic motion that take place within similar time scales, can be looked upon and followed over a finite time interval. This permits us to penetrate into the mechanism of the mutual damping that gives rise to both resonance and single-particle broadening in the course of the combined evolution and learn about the relative importance of the microscopic events that may compete in the selected approximation. Owing to the advent of nuclear transport processes (as observed, for example, when low energy collisions take place between heavy ions) it is nowadays a familiar issue to think about several features of nuclear dynamics in terms of nonequilibrium evolution in many body systems.[25] Most studies in this direction are concerned with the problem of nuclear friction or dissipation of large amplitude collective motion,[25] usually formulated in terms of classical master or Fokker-Planck equations that describe the relaxation of the macroscopic degree of freedom in the presence of a static intrinsic heat bath. Giant resonances should be regarded as quantal, rather than classical, harmonic oscillations, since their frequencies lie in the same range as the nucleonic orbital frequencies in the mean field, namely about a tenth of MeV. The theoretical description of their damping thus demands a proper approach on the basis of a parallel quantal treatment of both collective and particle dynamics. Such a standpoint leads to an attractive picture of the decay of this kind of collective excitation and gives rise, in a straightforward fashion, to a quantitative prediction for the damping width. This approach is indeed different from some recent works that consider single-particle dynamics as an important ingredient of nuclear dissipation[26–28] since our interest lies

on quantual high-frequency, rather than classical low-frequency, collective motion.

A realistic situation that may correspond to a finite nucleus poses several difficulties, starting from the necessity of stimulating the finite configuration space, or, equivalently, the distorted nuclear Fermi sphere, the delicate treatment demanded by angular momentum conservation, and the convenience of somehow renormalizing the coupling of the resonance to other collective, mainly surface, oscillations, considering, for example, the nucleon effective mass to be a function of the energy.[29] However, the relevant dynamical features of the situation under scope can be cast into a simplified model consisting of a quantal oscillator that undergoes Brownian motion in a fermionic environment of thermally excited and equilibrated nuclear matter.

The framework of the formulation is shown in Sec. II, where apart from a minimum of equations that display the major components of the calculations, most room is devoted to examining the different microscopic processes that draw the combined motion towards equilibration and that represent either phonon or particle-hole creation, propagation, and annihilation in a dynamical picture. They are represented by suitable diagrams. We briefly indicate how one can operate with graphs to extract the equations of motion for the bosonic density, that acquires the form of a Pauli-type master equation whose dynamics does not resemble the well-known classical macroscopic nuclear motion. It rather looks like the evolution of a linear chain with nearest neighbor interactions and asymmetric, temperature-dependent transition rates that are here rigorously derived within the frame of the model. The asymptotic motion of the fermion density is examined in Sec. III. It can be seen to respond to a modified kinetic equation, whose approach to equilibrium is governed by two kinds of collision frequencies, associated with the fermionic pairwise interaction and to the boson-fermion residual interaction, respectively.

Section IV contains our calculations performed in the oversimplified situation in which the heat reservoir remains at a steady state. This configuration naturally occurs in the sharp-resonance or energy-conserving version of intermediate propagation between consecutive collisions. The numerical analysis is carried out solving the eigenvalue problem of the master equation for the oscillator density. A range of temperature and phonon energies is considered, and the smooth behavior encountered allows straightforward extrapolations. The time evolution of the density is studied and quantitative estimates of the lifetime of an excited state or inverse width are given. Section V contains a discussion of the results while the summary and conclusions are presented in Sec. VI.

II. THE MODEL

A simplified model of the coupling between a quantal nuclear vibration and the fermionic environment consists of a harmonic oscillator with frequency Ω in contact with nuclear matter that provides a heat reservoir. The latter is assumed to be a fourfold (spin-isospin) degenerate Fermi gas whose equilibrium distribution at temperature T (MeV) is

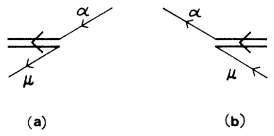

FIG. 1. Interaction vertices. (a) Phonon creation with particle deexcitation from orbital $|\alpha\rangle$ to orbital $|\mu\rangle$; (b) phonon annihilation with particle excitation from state $|\mu\rangle$ into $|\alpha\rangle$.

$$\rho_{\rm eq}=1/[1+\exp(\epsilon-\epsilon_F)/T] \ . \tag{2.1}$$

The overall system is assigned a Hamiltonian,

$$H=H_B+H_F+H_{BF} \ , \tag{2.2}$$

where the labels B, F, and BF stand for bosonic (collective), for fermionic, and for interaction, respectively. The latter is selected as a standard particle-phonon field of the form

$$H_{BF}=\sum_{\alpha\mu}(\lambda_{\alpha\mu}\Gamma^\dagger b_\mu^\dagger b_\alpha+\lambda^*_{\alpha\mu}\Gamma b_\alpha^\dagger b_\mu) \ . \tag{2.3}$$

In (2.3) the boson operators $\Gamma,\Gamma^\dagger$ are raising and lowering ones for quanta in the harmonic field, while $b^\dagger,b$ denote fermion creation and annihilation, respectively. We choose the labels α,β, etc., to specify single-particle (s.p.) states on top of the Fermi level, their deexcitation towards a single-hole state μ,ν, etc., is accompanied by the creation of a single phonon of energy $\hbar\Omega$, according to (2.3). The conjugate process (quanta annihilation) gives rise to a particle-hole pair. The interaction vertices are illustrated in Fig. 1. More generally, we later relax the restriction to states above and below the Fermi level, and speak instead of excited and deexcited s.p. orbitals. In this frame the term particle (hole) will be rather loosely used to denote those s.p. states that may release (accept) energy in order to create (destroy) a phonon.

We notice that the problem described by the Hamiltonian (2.2) plus the interaction (2.3) is formally identical to that of radiation-atom coupling in quantum optics (see, for example, Ref. 34). It should be borne in mind that a fundamental difference arises since the collective mode possesses a microscopic structure in terms of coherent particle-hole excitations.[3,4] This structure induces particle-phonon correlations that may not be ignored when analyzing finite nuclei. For our current purposes, those correlations are ignored; we defer to a later work the examination of their importance in spherical nuclei. Thus the present model considers an oscillator placed in a fermionic heat reservoir without any reference to its microscopic constitution.

The coupled equations of motion for the density matrices of the oscillator and the heat bath can be derived following established prescriptions of irreversible statistical mechanics, like the projection method of the theory of master equations[31–38] or the reduction technique that leads, for example, to the Bogoliubov-Born-Green-Kirkwood-Yvon (BBGKY) hierarchy and to the one-body

kinetic equation.[30,33] Either procedure yields formally the same result, differing perhaps in the representation of the correlation superpropagator U_{cc} defined below. We will not get into the details of the derivation; they are reviewed in Ref. 39. We simply quote here that we have decomposed the whole density vector as

$$\rho(t)=\rho_B(t)\rho_F(t)+\rho_c(t) =\rho_0(t)+\rho_c(t) , \tag{2.4}$$

where $\rho_0(t)$ is the state supervector of the vacuum or situation of statistical independence between the oscillator and its environment, and $\rho_c(t)$ is the correlation supervector belonging to the class of traceless supervectors with respect to both the fermion and boson coordinates. In this frame, the reduced equations of motion are obtained from the Liouville one,

$$i\hbar\dot{\rho}=L\rho=[H,\rho] , \tag{2.5}$$

utilizing either technique mentioned above. The final result takes the form of a causal evolution law,

$$i\hbar\dot{\rho}_Q=\mathscr{L}_Q\rho_Q+K_Q(\rho_0), \quad (Q=B,F) \tag{2.6}$$

where $\mathscr{L}_Q$ is the free-flow generator or effective Liouvillian,

$$\mathscr{L}_Q=L_Q+T_{-Q}(L_{BF}\rho_{-Q}) \tag{2.7}$$

(here $-Q$ denotes the complement of the coordinates labeled Q, and T is the symbol for a trace operation with respect to the variables in the subscript), the term K_Q is the collisional derivative,

$$K_Q(\rho_0)=\int_0^\infty d\tau T_{-Q}[\Psi_{BF}(\tau)\rho_0(t-\tau)] , \tag{2.8}$$

and Ψ_{BF} is the collision (or memory) superoperator,

$$\Psi_{BF}(\tau)=L_{BF}U_{cc}(\tau)L_{BF} . \tag{2.9}$$

Here U_{cc} is the superpropagator in correlation space, whose expression may look different according to the realization of the projection or reduction superoperator chosen to carry out the derivation. However, seemingly different expressions of U_{cc} are indeed equivalent except for, at most, a time-dependent phase factor. As an example, we note that the reduction procedure carried over by the scalar product in Liouville space that consists of tracing away the uninteresting degrees of freedom [T_{-Q} in Eq. (2.7)] gives in our case,[39]

$$U_{cc}(t)=\exp\left[-\frac{i}{\hbar}\int_0^t d\tau(1-\rho_F T_F-\rho_B T_B)L\right] , \tag{2.10}$$

while the time-independent projection proposed by Willis and Picard[40] gives, in our notation,

$$U_{cc}^{\mathrm{WP}}(t)=\exp\left[-\frac{i}{\hbar}\int_0^t d\tau(1-\rho_F T_F-\rho_B T_B +\rho_F\rho_B T_F T_B)L\right] . \tag{2.11}$$

It is clear that the exponents, operating on any Liouville vector, yield the same result, since they only differ in a total trace of a commutator, i.e.,

$$T_F T_B L(B,F)\rho(B,F)=T_F T_B[H(B,F)\rho(B,F) -\rho(B,F)H(B,F)]=0 .$$

We briefly recall the significance of the entities in Eqs. (2.7)–(2.9). The trace term in (2.7) represents the mean field that each subsystem experiences, on the average, due to the presence of its partner. The collision term given in (2.8) provides the dynamical coupling between both density supervectors that leads to mutual equilibration. The collision superoperator Ψ_{BF} is most often discussed in irreversible statistical mechanics,[30–33,37–39] where it is recognized as the irreducible kernel that causes vacuum-to-vacuum transitions through an infinite sequence of events in correlation space. For a review of the properties of the operators of kinetic theory, we refer the reader to Refs. 33 and 39 and references cited therein. Furthermore, we recall that the reduced density ρ_Q ($Q=B$ or F) remains normalized provided that $T_Q K_Q(\rho_0)=0$ at any time; this is a consistency requirement that one should check whenever a specific form of (2.8) is used.

In this work we have evaluated the non-Hermitian generators of the motion displayed in Eq. (2.6) for $Q=B$ and $Q=F$, in the weak coupling approximation[30–39] that consists of the choice, for the correlated superpropagator,

$$U_{cc}(\tau)\approx U_0(\tau)=\exp\left[-\frac{i}{\hbar}(L_B+L_F)\tau\right] , \tag{2.12}$$

i.e., the free superpropagator. The use of this approximation is legitimated under a set of conditions; first, the magnitude of the interaction strength must be small relative to a typical energy or frequency of the motion. This is satisfied in the nuclear problem where one expects the interaction strength $\lambda_{\alpha\mu}$ of Eq. (2.3) to be about or below 1 MeV for a giant-dipole mode of about 15 MeV of excitation energy in medium-heavy nuclei (see for example, the estimate given by Broglia[16] or Ref. 4, Chap. 6). Second, the interaction time must be sufficiently long for the energy to be conserved during the collision. Notice that hypothesis (2.12) combined with (2.9) and with the identity $\rho_0(t-\tau)=U_0(-\tau)\rho_0(t)$ leads one to calculating the time integral

$$\int_0^\infty d\tau\exp[i(\Omega-\omega_{\alpha\mu})t]=\pi\delta_+(\Omega-\omega_{\alpha\mu}) =\pi\delta(\Omega-\omega_{\alpha\mu}) +i\mathscr{P}[1/(\Omega-\omega_{\alpha\mu})] , \tag{2.13}$$

where $\hbar(\Omega-\omega_{\alpha\mu})$ is the energy variation as the interaction takes place. We use $\hbar\omega_{\alpha\mu}=\epsilon_\alpha-\epsilon_\mu$ for the transition energy of the pair $(\alpha\mu)$ in Eq. (2.3).

The details of the calculation are given in Ref. 39 and we quote the results in a diagrammatic representation whose ingredients are, in the Liouville space:[43]

(a) An arrowed double line denotes an oscillator Liouville state $|n\rangle\langle n'|$;

(b) Arrowed single lines designed *above* the phonon line are "excited" states, $|\alpha\rangle\langle\alpha'|$;

(c) Arrowed single lines drawn *below* the phonon lines

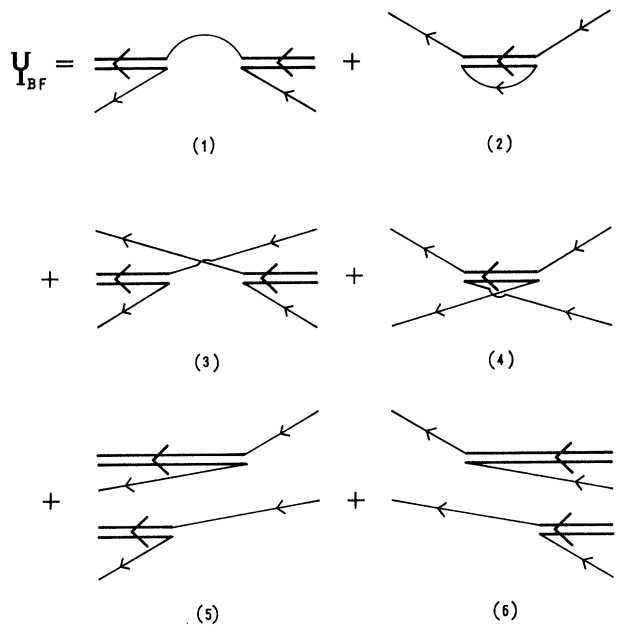

FIG. 2. Collision superoperator. See text for the description of the different graphs.

are "deexcited" states, $|\mu\rangle\langle\mu'|$.

Time always flows from right to left in every graph. We remark that in the present language, "excited" and "deexcited" s.p. states are relative concepts since they refer to the result of the annihilation of an oscillator quantum, or to its creation. In this frame, Ψ_{BF} is depicted in Fig. 2.

This figure symbolically exhibits six different kinds of processes carried out by the collision superoperator, between the initial and final vacuum configurations.

(1) Number-of-quanta-conserving processes with one less active phonon in the intermediate state accompanied by one propagating "excited" fermion;

(2) Number-of-quanta-conserving processes with one more phonon plus one propagating "deexcited" fermion;

(3) and (4) Conserving processes with one propagating p-h pair and either none or one active phonon in the intermediate state;

(5) and (6) Nonconserving processes, characterized by the creation of two extra quanta. Here the intermediate state consists of one propagating phonon plus one "excited" and one "deexcited" particles.

The collision derivatives are evaluated combining the diagrammatic representation of the collision kernel (Fig. 2) with the cluster structure of the many-fermion system. Observation of Fig. 2 permits us to discriminate three classes of initial vacuum states.

(a) Graphs (1) and (2) select those initial states that consist of a single fermion coexisting with the oscillator in state

$$\rho_B(t)=\sum \rho_{nn'}(t)\,|\,n\rangle\langle n'\,|\ .$$

In other words, $\rho_F(t)$ contributes just a one-particle cluster with weight

$$\rho_1(t)\equiv\rho(t)=\sum \rho_{AA'}(t)\,|\,A\rangle\langle A'\,|\ .$$

(b) Graphs (3) and (4) demand a two-fermion state on the right, represented by a two-cluster $\rho_2(1,2;t)$. We see that fermions belong to different classes, since one of them is assigned to create a phonon, while the other one will participate in quantum annihilation.

(c) Graphs (5) and (6) operate upon two-fermion states as well, but of the same kind, i.e., either both "excited" or "deexcited," since the collision process embodies two quanta creation or annihilation.

In the very-close-to-equilibration regime, where both ρ_B and the one-body component $\rho\equiv\rho_1$ of ρ_F are diagonal in their respective spaces these derivatives adopt the form,

$$K_B\sim\sum_{n\alpha\mu}|\,\lambda_{\alpha\mu}\,|^2\pi\delta(\Omega-\omega_{\alpha\mu})\,|\,n\rangle\langle n\,|\,\{\rho_{nn}[\rho_\mu(1-\rho_\alpha)+\rho_\alpha(1-\rho_\mu)]-\rho_{n-1,n-1}\rho_\alpha(1-\rho_\mu)-\rho_{n+1,n+1}\rho_\mu(1-\rho_\alpha)\}\ , \tag{2.14a}$$

$$K_F\sim\sum_{\alpha\mu}|\,\lambda_{\alpha\mu}\,|^2\pi\delta(\Omega-\omega_{\alpha\mu})\{\,|\,\mu\rangle\langle\mu\,|\,[(1-\rho_{00})\rho_\mu(1-\rho_\alpha\,|\,\alpha\rangle\langle\alpha\,|\,)-(1-\rho_{NN})\rho_\alpha(1-\rho_\mu\,|\,\alpha\rangle\langle\alpha\,|\,)]$$
$$+\,|\,\alpha\rangle\langle\alpha\,|\,[(1-\rho_{NN})\rho_\alpha(1-\rho_\mu\,|\,\mu\rangle\langle\mu\,|\,)-(1-\rho_{00})\rho_\mu(1-\rho_\alpha\,|\,\mu\rangle\langle\mu\,|\,)]\}\ . \tag{2.14b}$$

The conservative flow terms $\mathscr{L}_Q\rho_Q$ vanish in the asymptotic regime. The dissipative evolution of the matrix elements $\rho_{nn}\equiv\rho_n$ of ρ_B is governed by an asymmetric Pauli-type master equation,

$$\dot\rho_n=W_+(\rho_{n+1}-\rho_n)+W_-(\rho_{n-1}-\rho_n),\quad 0<n<N \tag{2.15a}$$

$$\dot\rho_0=W_+\rho_1-W_-\rho_0\ , \tag{2.15b}$$

$$\dot\rho_N=-W_+\rho_N+W_-\rho_{N-1}\ . \tag{2.15c}$$

Equations (2.15b) and (2.15c) express the fact that the oscillator spectrum is bounded (the upper bound at $n=N$ is here set for calculational purposes); consequently, one cannot accept probability flow from $n=0$ ($n=N$) other than towards $n=1$ ($n=N-1$). In this respect, the evolution problem posed by Eqs. (2.15) is that of a finite linear chain with nearest neighbor interactions and perfectly reflecting walls; notice that the same equation, considered to be valid for all n, describes the dynamics of the same chain with absorbing walls, i.e., the norm $T_B\rho_B$ is not a constant of the motion.

The upwards and downwards transition probabilities are, respectively,

$$\hbar W_+=\sum_{\alpha\mu}|\,\lambda_{\alpha\mu}\,|^2\pi\delta(\Omega-\omega_{\alpha\mu})\rho_\mu(1-\rho_\alpha) \tag{2.16a}$$

and

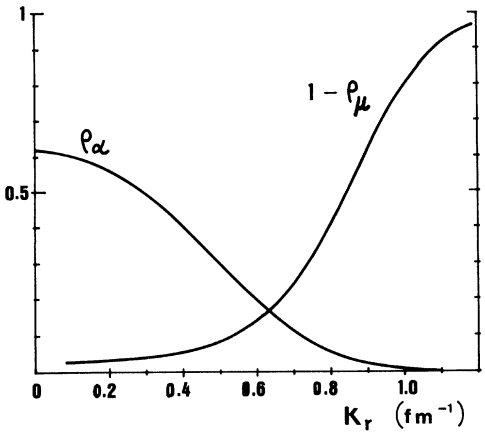

FIG. 3. Fermion occupation numbers in the summands for the transition rate W_-. They correspond to the computations undertaken in this work for a temperature $T=4$ MeV and a phonon energy $\hbar\Omega=18$ MeV. The abscissa is the radial momentum in fm^{-1}, since the other two components have added up according to the discussion in Sec. IV.

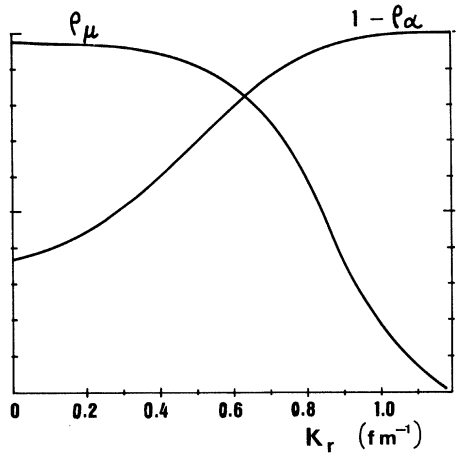

FIG. 4. Same as in Fig. 3 for the transition rate W_+.

$$\hbar W_- = \sum_{\alpha\mu} |\lambda_{\alpha\mu}|^2 \pi\delta(\Omega-\omega_{\alpha\mu})\rho_\alpha(1-\rho_\mu) \ . \tag{2.16b}$$

These expressions give the rate of gain (loss) of population of the oscillator state $|n\rangle\langle n|$ as a sum over transition strengths times the occupation probability of the fermion pair involved in the process $n\pm1$ quantum. If ρ_μ,ρ_α are close to Fermi distribution factors at a given temperature T, an estimate of the relative behavior of W_+ and W_- can be given; assuming $\rho_\mu\equiv\rho(\epsilon_\mu)$, we have $\rho_\alpha=\rho(\hbar\Omega+\epsilon_\alpha)$ due to energy conservation. The summands in Eqs. (2.16) are quantitatively drawn in Figs. 3 and 4 except for the transition strengths $|\lambda_{\alpha\mu}|^2$. According to this scheme, low temperatures ($T\ll\hbar\Omega$) favor W_+ and thus the evolution proceeds towards the oscillator ground state. Increasing temperature causes W_+ and W_- to become comparable; in this case, Eqs. (2.15) indicate that the motion is diffusionlike, rather than dissipative as in the former case.

The generator of dissipative-diffusive evolution is represented by an asymmetric tridiagonal matrix; in the present work,[39] the transition probabilities are neither postulated nor written down on heuristic grounds, but derived from the microscopic analysis of the generator of dissipative evolution in the general equation of motion (2.6). It is interesting to quote here that analytic expressions are available for the eigenvalues and eigenfunctions of such a matrix. They are given in the Appendix. Future calculations will rely heavily on the properties of these eigenvalues, whose evaluation demands the introduction of the fermion one-body densities in equilibrium.

III. RELAXATION OF THE MULTIFERMION SYSTEM

Before facing a model study of the master equation (2.15) we must establish some simplified form for the nucleon occupation probabilities $\rho_\alpha(t)$ or $\rho_\mu(t)$. Their asymptotic evolution demands some further work, since K_F in Eq. (2.14b) affects the motion of the whole N-body fermion density ρ_F. However, it is straightforward to show[41] that, starting from the general equation of irreversible motion (2.6), for $Q=F$, the reduction procedure that builds up the well-known BBGKY equation[30,33] gives rise to a "modified BBGKY hierarchy" that includes the coupling mechanism with both a conservative and a dissipative contribution. Noticing that K_F in Eq. (2.14b) is the sum of a one-body plus a two-body term,

$$K_F(\rho_0)=K_0\rho+K_1\rho_2^{(0)} \ , \tag{3.1}$$

where $\rho_2^{(0)}(1,2)$ is the antisymmetrized two-fermion density, one arrives at a modified kinetic equation that reads

$$i\hbar\dot{\rho}=\mathscr{L}^M\rho+iK^M\rho \ , \tag{3.2}$$

with

$$\mathscr{L}^M(1)=\mathscr{L}^{\rm KIN}(1)+T_B[L_{BF}(1)\rho_B] \ , \tag{3.3a}$$

$$K^M(1)=K_0(1)+Tr_2K_1^A(1,2)\rho(2)+K^{\rm KIN}(1) \ . \tag{3.3b}$$

Equation (3.2) displays the standard structure of a kinetic equation,[33] while both the Hermitian, free-flow generator $\mathscr{L}^M$ and the dissipative kernel K^M exhibit the boson-averaged effect of the external coupling agent. The superscript KIN denotes the kinetic contribution to either conservative or dissipative dynamics, the corresponding generators being, respectively, the Hartree-Fock Liouvillian

$$\mathscr{L}^{\rm KIN}(1)=[\mathscr{H}_{\rm HF}(1), \ ]$$
$$=[h_0(1)+Tr_2V(1,2)\rho(2), \ ]$$

and the Boltzmann collision kernel $K^{\rm KIN}$ whose expression has been written down by many authors (see Refs. 30 and 33 and references therein).

For several applications, it is useful to dispose of a diagrammatic representation for K_F. We introduce thus the collision vertices as depicted in Fig. 5 where lines denote either Liouville states $|A\rangle\langle A'|$ or particle labels 1,2; the wiggly lines indicate antisymmetrization between the particle lines they link. Figure 5(a) corresponds to K_0 in Eq. (3.1), while Fig. 5(b) represents K_1. Within this scheme an

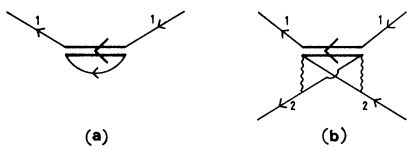

FIG. 5. One and two fermion collisional vertices [(a) and (b), respectively]. The wiggly lines denote antisymmetrization of the two-particle wave function in both the initial and final state.

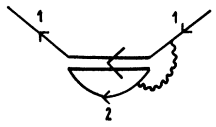

FIG. 6. Diagrammatic expansion of the modified collision term of the fermionic heat bath. See text for the description of the graph.

object like $\mathrm{Tr}_2 K_1(1,2)\rho(2)$ that appears in the modified collision derivative (3.3b) is drawn in Fig. 6. It should be remarked that the presence of the wiggly line tells us that the particle line in the intermediate state carries a relative weight $\rho(2)$ (either a matrix element $\rho_{\alpha\alpha'}$ or $\rho_{\mu\mu'}$), while the simple one-body collision vertex 5(a) is weighted by a Kronecker delta in the given indices. The whole modified collision kernel can be diagrammatically written as the sum of the drawings in Figs. 6 and 5(a) plus the kinetic term[30,33] proportional to the square of the fermion pair-wise interaction, $([V,\ ])^2$. Its expression in the current regime has been worked out in Ref. 30 and calculations of the mean free paths associated with this kernel have been performed in Ref. 42 for different nuclear interactions.

In the very-close-to-equilibration regime, the fermions in the heat bath obey the linearized kinetic equation,[41]

$$\hbar\dot{\rho}(1)=[-i\mathscr{L}^{\mathrm{KIN}}(1)+\mathscr{K}^{\mathrm{KIN}}(1)+\mathscr{K}_{\mathrm{OSC}}(1)]\rho(1)\ . \tag{3.4}$$

The expression for $\mathscr{K}^{\mathrm{KIN}}(1)$ is given in Ref. 30 while for $\mathscr{K}_{\mathrm{OSC}}$ we get

$$\mathscr{K}_{\mathrm{OSC}}=\sum_{\alpha\mu}|\lambda_{\alpha\mu}|^2\pi\delta(\Omega-\omega_{\alpha\mu})\{[(1-\rho_0)\rho_\mu(1-\rho_\alpha)-(1-\rho_N)\rho_\alpha(1-\rho_\mu)]\,|\mu\rangle\langle\mu|$$
$$+[(1-\rho_N)\rho_\alpha(1-\rho_\mu)-(1-\rho_0)\rho_\mu(1-\rho_\alpha)]\,|\alpha\rangle\langle\alpha|\}\ . \tag{3.5}$$

The Hartree-Fock or conservative term $\mathscr{L}^{\mathrm{KIN}}(1)$ is zero when $\rho(1)$ is diagonal.

The total collision frequencies are then the eigenvalues of the superoperator $\mathscr{K}_{\mathrm{TOT}}=\mathscr{K}_{\mathrm{KIN}}+\mathscr{K}_{\mathrm{OSC}}$. Since the diagonalization problem here involved represents a rather heavy numerical task, if even possible, we resort to the relaxation time approximation[33,41,42]; we assume that the occupation number of the state $|A\rangle\langle A|$ is

$$\rho_A(t)=\rho_A(eq)+\delta\rho_A(t)\ , \tag{3.6}$$

where

$$\delta\dot{\rho}_A(t)=-\delta\rho_A(t)/\tau_{\mathrm{TOT}}(A)=-\nu_{\mathrm{TOT}}(A)\delta\rho_A(t)\ . \tag{3.7}$$

Here $\nu_{\mathrm{TOT}}=\tau_{\mathrm{TOT}}^{-1}$ is taken as the sum of the representative estimates of the respective kernels. The kinetic frequencies ν_{KIN} are well known;[42] for the remaining contributions we select the same approach that gives rise to them.[33,41,42] It consists of linearizing the loss (positive) term in the kernels. We obtain the expression

$$\hbar\nu_{\mathrm{OSC}}(A)=\sum_{\alpha\mu}|\lambda_{\alpha\mu}|^2\pi\delta(\Omega-\omega_{\alpha\mu})$$
$$\times\{(1-\rho_0)[1-\rho_\alpha(eq)]\delta_{A\mu}$$
$$+(1-\rho_N)[1-\rho_\mu(eq)]\delta_{A\alpha}\}\ . \tag{3.8}$$

At this point a feature of the model shows up as follows. Since the transition vertices V_{BF} must satisfy momentum conservation, we actually have

$$\lambda_{\alpha\mu}=\lambda^0_{\alpha\mu}\delta(\vec{q}-\vec{k}_{\alpha\mu})\ , \tag{3.9}$$

with $\vec{q},\vec{k}_{\alpha\mu}$ the phonon and relative fermion momenta, respectively. The summation over s.p. labels is, in the thermodynamic limit,

$$\sum_A=\hbar g\int d^3k_A\ , \tag{3.10}$$

where g is the total momentum degeneracy, including the spin-isospin degrees of freedom. If we assume that the boson energy and momentum satisfy a dispersion relation for acoustic modes,

$$\Omega=c_s|\vec{q}|=c_s q\ , \tag{3.11}$$

with c_s an average sound velocity of the fermion environment, we find for $\nu_{\mathrm{OSC}}(\mu)$ the expression,

$$\nu_{\mathrm{OSC}}(\vec{k}_\mu)=g|\lambda^0_{\vec{k}_\mu+\vec{q},\vec{k}_\mu}|^2[1-\rho_{\vec{k}_\mu+\vec{q}}(eq)]$$
$$\times\pi\delta\left[\frac{\hbar^2}{2m}(2k_z q+q^2)-\hbar c_s q\right]\ . \tag{3.12}$$

A similar form is valid for $\nu_{\mathrm{OSC}}(\vec{k}_\alpha)$. We recognize in (3.12) the combined effect of both energy and momentum conservation, that restricts the participation of "deexcited" fermion states to those lying in the plane

$$k_{z_\mu}=mc_s/\hbar-q/2\ . \tag{3.13}$$

The z axis is taken as parallel to the phonon momentum $\vec{q}$. Furthermore, for the "excited" particles it must hold,

$$k_{z_\alpha}=mc_s/\hbar+q/2\ , \tag{3.14}$$

the presence of the delta symbol in Eq. (3.12) must be un-

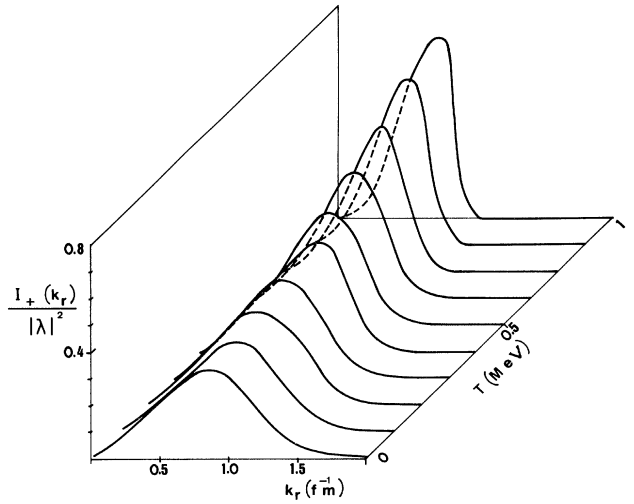

FIG. 7. Integrand of the transition rate W_+ as a function of temperature (in MeV) and radial momentum (in fm^{-1}).

derstood as indicating a limiting situation, corresponding to perfectly elastic nucleon-oscillator collisions. The better energy is conserved during the interaction, the larger the collision frequency whose elastic limit is symbolically written down in Eq. (3.12). It further indicates that the oscillator will be ignored by those fermions lying outside the planes (3.13) or (3.14) in momentum space. The dynamics of these planes is fairly interesting, since it takes place with an infinite total collision frequency, or zero relaxation time. It means that while the rest of the heat bath remains in the thermodynamic state previous to the particle-phonon collision, these fermionic planes are instantaneously thermalized, acquiring without delay an equilibrium temperature that could be related, using a bidimensional Fermi gas model, to the excitation energy given up by the oscillator. Overall thermalization of the fermion system takes place via particle-particle collisions with a finite relaxation time,

$$\tau_{\rm KIN}^{-1}(A)=\nu_{\rm KIN}(A) \ . \tag{3.15}$$

The sudden equilibration of the momentum space subsets (3.13) and (3.14) is a model characteristic related to the appearance of a sharp resonance. The energy-conserving distribution $\delta(\Omega-\omega_{\vec{k}_\mu+\vec{q},\vec{k}_\mu})$ is the time integral of an uncorrelated propagator for the combined system. If the spreading width of the harmonic mode were included in the form of a lifetime Δ^{-1} for the evolution kernel U_{cc} [see Eqs. (2.6)–(2.10)], a Lorentzian function of width Δ would take the role of the energy-conserving filter. In such a case, of course, $\nu_{\rm OSC}(A)$ would remain finite, although larger for those fermions with momentum pointing to the planes discussed above.

A quantitative comparison between the kinetic frequency $\nu_{\rm KIN}$ and the oscillator-induced correction $\nu_{\rm OSC}$ depends upon the magnitude of the coupling strengths $\lambda_{a\mu}$. Since in this work, it stands as an arbitrary parameter, further statements are deferred until the model is applied to a semirealistic situation, i.e., a finite nucleus.

IV. QUANTITATIVE ANALYSIS OF THE MASTER EQUATION

We are now solving the master equation (2.15) that gives the evolution of the occupation probabilities of the oscillator levels. The transition rates W_+ and W_- in Eqs. (2.16) take the form,

$$W_+=2\pi^2 g^2 \int dk_{r_\mu} k_{r_\mu} |\lambda(k_{r_\mu},q)|^2 \rho(k_\mu)[1-\rho(k_\mu,q)] \ , \tag{4.1a}$$

$$W_-=2\pi^2 g^2 \int dk_{r_\mu} k_{r_\mu} |\lambda(k_{r_\mu},q)|^2 \rho(k_\mu,q)[1-\rho(k_\mu)] \ . \tag{4.1b}$$

These expressions arise after integration of the momentum and energy conservation filters, under the simplifying assumption that the transition strength λ is isotropic. The only remaining integration variable is the radial momentum component in the interacting subsets (3.13) and (3.14). Although the general derivation of the transition rates allows for the overall time dependence of the fermion density, the analysis of $\nu_{\rm TOT}(\mu)$ in the preceding section establishes that the participating $\rho(\vec{k}_\mu),\rho(\vec{k}_\alpha)$ are static ones, corresponding to thermal equilibrium of a Fermi gas at temperature T.

Calculations are performed for the case $\lambda=cte$. This implies that all computed frequencies are given in units MeV^2 $(10^{-21}$ sec$)^{-1}/|\lambda^2|$. Assuming a phonon dispersion relation (3.11) for acoustic modes in the nuclear fluid, we evaluate the transition rates W_+ and W_- for a range of phonon frequencies that represents a typical fringe of giant dipole resonance (isovector) energies, i.e., from 13 to 18 MeV. A wide interval of temperatures is selected in order to dispose of an ample scope of the behavior of the interesting quantities. As an example, the integrand of Eq. (4.1a) is displayed in Fig. 7, as a function of radial momentum k_r (in fm^{-1}) and temperature T (MeV). It corresponds to a phonon energy $\hbar\Omega=13$ MeV. We see how the filter shape of this integrand is modified in a drift-plus-diffusion fashion with increasing temperature; while the width grows from about 0.4 to 0.8 fm^{-1}, the centers slightly move between 0.75 and 0.85 fm^{-1}. Taking an average value for the energy associated to the peak, we find,

$$\bar{\epsilon}_\mu=\epsilon(k_{r_\mu}=0.8 \text{ fm}^{-1}) = 32.55 \text{ MeV} \ . \tag{4.2}$$

In our calculations, the Fermi energy is 38 MeV.

The transition rates W_+ and W_- are displayed in Figs. 8 and 9, respectively, as functions of both temperature and phonon energy. They have been computed using a Gauss-Legendre algorithm combined with a convenient truncation of the semi-infinite energy domain. The overall behavior reproduces the features expected on qualitative grounds. While the general trend of W_+ is to decrease with increasing temperature and smaller phonon energy, W_- shows the complementary behavior. The ratio W_-/W_+ is predominantly governed by the tempera-

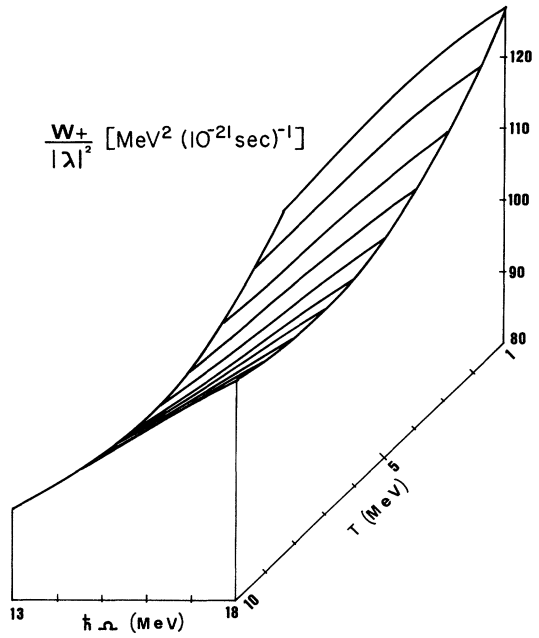

FIG. 8. Transition rate W_+ in units of the squared interaction strength $|\lambda|^2$ as a function of temperature and phonon energy in MeV.

ture and it ranges between 10^{-7} for $T=1$ MeV and about 0.2 for $T=10$ MeV, in the middle of the energy interval. This means that in the investigated parameter domain, the evolution given by the master equation will be dominated by W_+, that gives the rate of population of state $|n\rangle\langle n|$ from the decay of the high-lying near neighbor.

The time evolution of the boson density matrix can be easily examined with the help of an expansion with respect to the eigenfunctions of the matrix Eq. (2.15), of the form

$$\rho(t)=\sum_{l=1}^{N} c_l V^{(l)} e^{-\lambda_l t} , \tag{4.3}$$

for the vector with components $\rho_n(t)$. Recalling that the eigenvectors, $V^{(l)}$, other than the equilibrium solution $V^{(1)}=\rho^{(0)}$ are traceless vectors, we see that the condition $\mathrm{Tr}\rho(0)=1$ demands the coefficient of $\rho^{(0)}$ in (4.3) to be equal to unity. Accordingly,

$$\rho(t)=\rho^{(0)}+\sum_{l=2}^{N} c_l V^{(l)} e^{-\lambda_l t} , \tag{4.4}$$

from where we verify the asymptotic condition $\rho(t)\to\rho^{(0)}$ as $t\to\infty$.

Owing to the orthogonality between the eigenvectors $V^{(l)}$ and those of the adjoint problem (see Appendix), the coefficients c_l can be determined as

$$c_l=V^{\dagger(l)}\cdot\rho(0) . \tag{4.5}$$

Correspondingly, we introduce the adjoint density $\rho^\dagger$ as

$$\rho^\dagger=\rho^{\dagger(0)}+\sum_{l=2}^{N} c_l V^{\dagger(l)} e^{-\lambda_l t} . \tag{4.6}$$

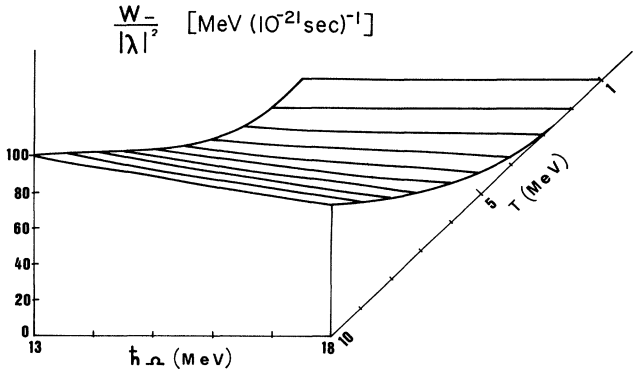

FIG. 9. Same as in Fig. 8 for the transition rate W_-.

The expressions of the eigenvalues λ_l and the eigenvectors $\rho^{(0)}, V^{(l)}$ and their adjoints can be found in the Appendix with their derivations.

The following calculations have been performed assuming an initial condition $\rho_k(0)=\delta_{k1}$ that simulates, for example, photoabsorption excitation of a giant dipole resonance in spherical nuclei. The model space has been truncated at $N=7$ although we have verified that the general behavior of the figures is not sensitive to enlarging the given space. We have chosen several indicative parameters of the evolution:

(1) A center of gravity of the eigenvalues, or "mean frequency" $\bar{\nu}(t)$,

$$\bar{\nu}(t)=\frac{\rho^\dagger(t)\cdot[M\rho(t)]}{\rho^\dagger(t)\cdot\rho(t)} =\frac{\sum_{l=2}^{N} c_l^2\lambda_l e^{-2\lambda_l t}}{1+\sum_{l=2}^{N} c_l^2 e^{-2\lambda_l t}} . \tag{4.7}$$

(2) A center of gravity of the eigenvalues in the subspace orthogonal to the equilibrium eigenvector, or mean frequency $\bar{\nu}'$ associated to the perturbation $\delta\rho(t)=\rho(t)-\rho^{(0)}$,

$$\bar{\nu}'(t)=\frac{\sum_{l=2}^{N} c_l^2\lambda_l e^{-2\lambda_l t}}{\sum_{l=2}^{N} c_l^2 e^{-2\lambda_l t}} . \tag{4.8}$$

As seen from the definitions, for very long times $\bar{\nu}(t)$ will approach zero, while $\bar{\nu}'$ will evolve towards the lowest nonvanishing eigenvalue λ_2. This is illustrated in Fig. 10 where these quantities are displayed as a function of time for $T=5$ MeV. Here the time unit is the oscillator period, $2\pi/\Omega$, and the phonon energy is $\hbar\Omega=13$ MeV. In addition, a parameter for comparison is provided by the logarithmic derivative of the energy, $\nu_E(t)$,

$$\nu_E(t)=\frac{1}{E(t)}\frac{dE(t)}{dt} . \tag{4.9}$$

In Fig. 11 we exhibit (i) the eigenvalues λ_2, λ_4, and λ_5,

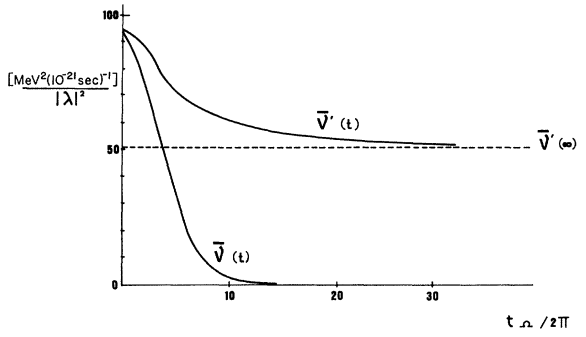

FIG. 10. Mean frequencies $\bar{\nu}$ and $\bar{\nu}'$ (in 10^{-21} $\sec^{-1}$) defined in Eqs. (8.6) and (8.7) as functions of time (in units of the oscillator period $T=2\pi/\Omega$). The temperature is 5 MeV, the phonon energy is 13 MeV.

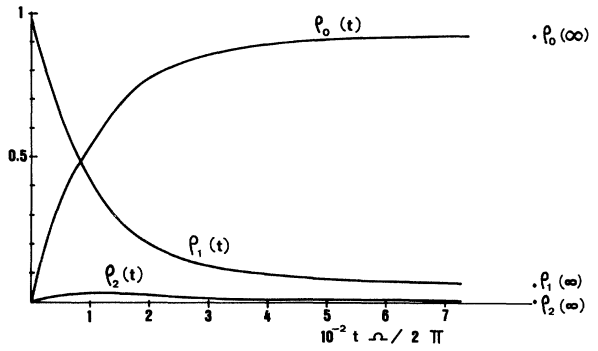

FIG. 12. First three components of the boson density vector as a function of a dimensioned time for the case $T=5$ MeV, $\hbar\Omega=13$ MeV, and $|\lambda|=1$ MeV.

(ii) the mean frequency $\bar{\nu}(0)$, (iii) the perturbed mean frequency $\bar{\nu}'(0)$, and (iv) $\nu_E(0)$. These quantities are plotted as a function of temperature, and correspond to $\hbar\Omega=13$ MeV. It can be observed that, within the resolution of the vertical scale, all these parameters coincide at $T=1$ MeV. In particular, the eigenvalues are $\lambda_2=97.52$, $\lambda_4=97.72$, and $\lambda_5=97.84$ in their corresponding units. The curves diverge from these points with increasing temperature, although the mean frequencies $\bar{\nu}$ and $\bar{\nu}'$ remain between the eigenvalues λ_4 and λ_5 over almost the whole range. Since $\bar{\nu}(0)$ and $\bar{\nu}'(0)$ give indication about the initial evolution trend of ρ and the perturbation $\delta\rho$, respectively, it is worthwhile noticing that for the selected initial condition, the largest expansion weights correspond to the eigenvectors number 4 and 5. This is indeed the case for temperatures up to 8 MeV; for larger temperatures, the contribution of these eigenvectors progressively decreases, causing the change in the slope of the curve $\bar{\nu}(0)$. A further illustration of the influence of the initial distribution on the dynamics is given by $\nu_E(0)$, that measure the initial decay tendency. It is seen from this figure that it remains, with the mean frequencies and the fourth and fifth eigenvalues, within a range of about twenty units along the vertical scale for temperatures below 3 MeV. The negative slope causes ν_E to depart from the other quantities for higher temperatures, reflecting the fact that the larger amount of population demanded by highly excited eigenstates slows down the initial rate of energy loss.

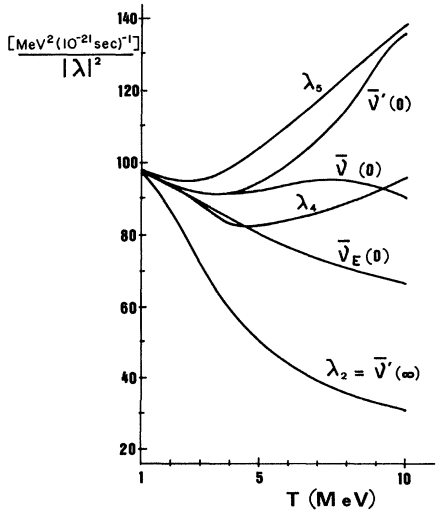

FIG. 11. Second, fourth, and fifth eigenvalues (ordered according to increasing magnitude) of the generator of motion M and the starting mean frequencies $\bar{\nu}$, $\bar{\nu}'$, and ν_E as functions of temperature for $\hbar\Omega=13$ MeV.

Finally, the evolution is displayed in Fig. 12 where the first three components of the density vector are shown as a function of time. They have been computed for $\hbar\Omega=13$ MeV and $T=5$ MeV. The exponential growth of $\rho_0(t)$ is clearly appreciated as well as the decay of ρ_1. The component ρ_2 is seen to grow to a low maximum and drops quickly to zero, while the remaining components cannot be shown in the current scale.

V. DISCUSSION

In the preceding section we have presented typical parameters and gross features of the time evolution of the phonon density vector. To this aim we have explicitly solved the previously derived master equation, whose transition rates have been computed on microscopic foundations. As shown earlier in this work, these transition rates W_+ and W_- depend on time and temperature through the fermion one-body densities that weight the availability of particle-hole pair states, required to host the result of phonon decay (or, to feed quanta creation in the conjugate process). Furthermore, the equilibrium distribution of phonons at temperature T is (see Appendix)

$$\rho_n^{(0)}(T)=C\left[\frac{W_-(T)}{W_+(T)}\right]^n, \tag{5.1}$$

where $W_\pm$ are chosen at their asymptotic values, if time dependent. In the present work, $W_\pm$ are constants since

the sharp-resonance approach (namely, the selection of a free propagator in intermediate states) freezes the evolution of the fermionic reservoir (see Sec. V). Equation (5.1) is just the canonical equilibrium distribution at temperature T, thus the ratio W_-/W_+ is proportional to the Boltzmann factor $\exp(-\hbar\Omega/T)$. This proportionality is verified under calculation, as already mentioned in connection with Figs. 8 and 9.

One could wonder about the minimum in $W_+(T)$ for a fixed value of $\hbar\Omega$ that can be observed in Fig. 8. It takes place between 6 and 7 MeV, for every phonon energy. In order to explain the necessity of such minima, we will consider the high temperature limit (Boltzmann limit), $T \gg \epsilon_F$. In this case, the Fermi distribution is just the classical one and the Pauli exclusion principle is not active. Thus we can write,

$$\rho(\vec{k}_\mu)[1-\rho(\vec{k}_\mu+\vec{q})] \approx \exp\left[-\frac{\epsilon_\mu-\epsilon_F}{T}\right] . \tag{5.2}$$

A glance at expressions (2.16) for the transition rates may convince the reader that in the limit (5.2), they become proportional to the exponential factor containing the energy in the participating planes k_z [Eqs. (3.13) and (3.14)], the proportionality factor being the radial integral, identical for both W_+ and W_-. Then

$$W_\mp = \exp\left[-\hbar^2\left[\frac{mcs}{\hbar} \mp \tfrac{1}{2}q\right]^2 \Big/ 2mT\right] 2\pi g^2 |\lambda|^2 I_r(T) , \tag{5.3}$$

where

$$I_r(T) = \int_0^\infty dk_{r_\mu} k_{r_\mu} \exp\left[-\left[\frac{\hbar^2 k_{r_\mu}^2}{2m} - \epsilon_F\right] \Big/ T\right]$$

$$= \exp(\epsilon_F/T)\frac{mT}{\hbar^2} . \tag{5.4}$$

Equations (5.3) and (5.4) show that both transition rates increase with temperature while their quotient approaches unity from below. For all values of T, W_- remains smaller than W_+ due to the Boltzmann ratio. This implies that the collective excitation associated with n quanta at $t=0$ will necessarily decay towards the equilibrium eigensolution; an external pump would be required to provoke any other kind of evolution. Now, since the low-temperature behavior of W_+ is governed by a negative slope dW_+/dT, due to the Pauli-controlled decrease of the values of its integrand (Fig. 8), it is clear that a minimum will take place in order to reach the high-temperature asymptote (5.3). We remark that in the present discussion, the concepts of high and low temperature are relative to the fermionic environment with typical temperature ϵ_F. Of course, the nuclear regime always corresponds to a degenerate Fermi gas ($T \ll \epsilon_F$) and for situations of physical interest, temperatures are confined to a small interval around 1 or 2 MeV. The calculations undertaken in this work just illustrate the smooth behavior of the quantities that rule this type of irreversible evolution.

The problem of time evolution of the boson density has been reduced, after solving the spectral problem for the generator of motion, to calculating an expansion of the form (4.3). It has been shown that the evolving density vector can be always written as

$$\rho(t) = \rho^{(0)} + \delta\rho(t) , \tag{5.5}$$

where $\rho^{(0)}$ is the equilibrium distribution at the given temperature and $\delta\rho(t)$ the decaying part whose amplitudes depend upon the initial conditions. It is clear from Eq. (5.4), as well as from the examination of the mean frequency $\bar{\nu}'(t)$, that the long-time behavior of $\delta\rho(t)$ is approximately exponential with a decay constant λ_2, namely the smallest nonvanishing eigenvalue of the evolution matrix. One could thus regard $\tau_B = \lambda_2^{-1}$ as the half-life of the excited collective mode; in such a frame, λ_2 just represents the width of the resolvent in energy space and should be proportional to the observed damping width of the harmonic coordinate.

VI. SUMMARY

In this work we have undertaken a study of the coupled dynamics of a boson system, consisting of a number of quanta that measure the excitation of an oscillator, and a multifermion system that provides a heat bath. Such a configuration is intended to give a rough representation of a collective mode in a large nucleus that decays via interaction with the nucleons; we choose then a boson-fermion coupling of the standard nuclear form.[39] Starting from the Liouville equation of motion, a reduction procedure permits us to describe the combined dynamics through two coupled equations that relate the oscillator and the fermion density vectors. A further reduction of the fermionic dynamics in a usual kinetic fashion[30,33] allows one to formulate the problem in terms of two coupled equations for the boson and the single-fermion densities. The latter is a modified kinetic equation, bearing the effect of the coupling through one extra contribution to the collision frequency. In other words, the presence of the oscillator produces a broadening of s.p. lines, in addition to that (usually low in nucleonic systems) due to two-particle collisions.

In order to fix the ideas with a solvable example, the details have been worked in a weak-coupling scheme; the collision superoperator, the collisional derivatives, and their close-to-equilibrium expressions have been analytically evaluated. It has been shown that the replacement of the intermediate propagator by an unperturbed one gives rise to a sharp-resonant effect, whose consequence is to provoke instantaneous thermalization of the fermionic subsets that participate in energy and momentum conserving collisions with the oscillator. This property permits us to write a simple master equation for the evolution of the boson system, considering that the fermion partners build up a heat reservoir in equilibrium at a given temperature T. This constitutes a question of vector evolution under a non-self-adjoint generator and can be tackled solving the spectral problem exactly. The solution and discussion of this eigenvalue subject have given rise to the preceding two sections in this work.

We must remark here that the smooth-behaved results displayed in Secs. IV and V correspond to an oversimplified situation; an infinite fermion system in thermal equilibrium inducing Brownian-type motion on a structureless oscillator. In order to describe a configuration that could better simulate the coupling of a nuclear collective mode to the remaining degrees of freedom, several limitations of this model should be raised. Rather than attempting a detailed microscopic calculation of the collisional derivatives, it should be interesting to consider the possibility of including, in an approximate way, some realistic effects. It is likely that one could reasonably simulate (a) the finite nuclear size in the manner of distortions on the Fermi sphere, (b) the boson-fermion correlations related to the microscopically coherent nature of the nuclear quantum, (c) the finite resonance width that accounts for a finite collision frequency for the fermions, and (d) the coupling to low-energy, surface collective modes as mass renormalization. We believe that the present simplified model, for which the elements of the general theory have been explicitly computed, provides a reference frame into which refinements could be inserted to adjust some of the features of the physical situations.

ACKNOWLEDGMENTS

The authors wish to acknowledge the Laboratorio de Física del Plasma at their home institution for access to their computing facilities. One of us (E.S.H.) is indebted to the Consejo Nacional de Investigaciones Científicas y Técnicas of Argentina (CONICET) for financial support. One of us (C.O.D.) is grateful to Dr. R. Depine, Dr. R. Mancini, and Dr. A. Banuelos for valuable aid with the computational task. This work was performed under Grant No. 9413/81 from CONICET, Argentina.

APPENDIX

We look at the spectral problem

$$MV^{(s)}=\lambda_s V^{(s)} , \tag{A1}$$

with the nonsymmetric tridiagonal matrix

$$M=\begin{bmatrix} -W_- & W_+ & & & & \\ W_- & -(W_-+W_+) & W_+ & & & \\ & \ddots & \ddots & \ddots & & \\ & & W_- & -(W_-+W_+) & W_+ & \\ & & & W_- & -W_+ \end{bmatrix} \tag{A2}$$

that generates the motion of the boson density according to the master equation (4.5). This matrix is trace nullifier, i.e., for any vector V,

$$\mathrm{Tr}(MV)=0 . \tag{A3}$$

Consequently,

$$\mathrm{Tr}(MV^{(s)})=\lambda_s \sum_{k=1}^{N} V_k^{(s)}=0 . \tag{A4}$$

In other words, the eigenvectors of the matrix M associated with nonzero eigenvalues are traceless vectors.

On the other hand, it can be seen that the determinant $\det(M)$ is equal to zero; this implies $\lambda_1=0$ is an eigenvalue. The corresponding eigenvector is the equilibrium solution $\rho^{(0)}$ and can be straightforwardly obtained with the ansatz

$$\rho_k^{(0)}=V_k^{(1)}=C_0\alpha^k , \tag{A5}$$

where C_0 is a normalization factor. Operating with M upon $\rho^{(0)}$ easily shows that

$$\alpha=\frac{W_-}{W_+} , \tag{A6}$$

in correspondence with the exact stationary solution of the master equation for systems in detailed balance discussed in Ref. 45.

As one writes down the coefficients of the secular equation $\det(M-\lambda I)=0$, one finds that the corresponding polynomial of Nth degree reads

$$P_N(\lambda)=-\lambda P'_{N-1}(\lambda) , \tag{A7}$$

with P' the secular polynomial for the $(N-1)$-dimensional matrix,

$$M'=\begin{bmatrix} -(W_-+W_+) & W_+ & & & \\ W_- & -(W_-+W_+) & W_+ & & \\ & W_- & -(W_-+W_+) & W_+ & \\ & & W_- & -(W_-+W_+) & \end{bmatrix} . \tag{A8}$$

We recognize the major difference between M and M'. Indeed while the former corresponds to a linear chain containing N nodes and fixed, reflecting walls at $n=1$, $n=N$, the latter describes the same situation with absorbing walls, since M' is not trace conserving as a generator of motion. In other words, if $\dot{\rho}=M'\rho$, $d(\mathrm{Tr}\rho)/dt$ does not vanish at all times. The advantage here is that the eigenvalue problem for M' is known[46] and the solution reads

$$\lambda_s=-(W_-+W_+)+2(W_-W_+)^{1/2}\cos\frac{s\pi}{N}\ , \qquad (s=1,\ldots,N-1)\ . \quad \text{(A9)}$$

It is straightforward to verify that the corresponding eigenvectors are

$$V_k'^{(s)}=\alpha^{k/2}\times\begin{cases}\sin\dfrac{ks\pi}{N}\\ \cos\dfrac{ks\pi}{N}\end{cases}\ . \quad \text{(A10)}$$

A simple expression can be found for the traceless eigenvectors of M with the ansatz

$$V_k^{(s)}=A_s\sin\frac{ks\pi}{N}+B_s\cos\frac{ks\pi}{N}\ . \quad \text{(A11)}$$

Placing (A11) into the spectral equation (A1) allows determination of A_s and B_s, that must be adjusted to satisfy the boundary conditions for reflecting walls contained in the first and last components of the vector $(M-\lambda_s I)V^{(s)}$. We easily obtain,

$$V_k^{(s)}=\alpha^{(k+1)/2}\sin\frac{ks\pi}{N}-\alpha^{k/2}\sin\frac{(k-1)s\pi}{N}\ . \quad \text{(A12)}$$

It is well known (see, for example, Ref. 45) that the eigenvectors $V^{\dagger(s)}$ of the adjoint problem

$$V^{\dagger(s)}M=\lambda_s V^{\dagger(s)}\ , \quad \text{(A13)}$$

are orthogonal to the V's, namely

$$\sum_{k=1}^{N}V_k^{\dagger(s)}V_k^{(s)}=0\ . \quad \text{(A14)}$$

These eigenvectors are computed with the same procedure as the V's, giving

$$V_k^{\dagger(s)}=\alpha^{-(k-1)/2}\sin\frac{ks\pi}{N}-\alpha^{-k/2}\sin\frac{(k-1)s\pi}{N}\ . \quad \text{(A15)}$$

The scalar product $V^{\dagger(s)}\cdot V^{(s)}$ is then used to normalize both vectors. In particular, the adjoint equilibrium solution is

$$\rho_k^{\dagger(0)}=V_k^{\dagger(1)}=C_0'\alpha^{-k}\ , \quad \text{(A16)}$$

and this, as well as $\rho^{(0)}$, are instead normalized according to the Liouville space metrics,

$$\mathrm{Tr}\rho^{(0)}=\mathrm{Tr}\rho^{\dagger(0)}=1\ . \quad \text{(A17)}$$

[1] G. E. Brown and M. Bolsterli, Phys. Rev. Lett. 3, 472 (1959).
[2] G. E. Brown, *Unified Theory of Nuclear Models and Forces* (North-Holland, Amsterdam, 1971), Chap. IV.
[3] J. M. Eisenberg and W. Greiner, *Nuclear Theory* (North-Holland, Amsterdam, 1972).
[4] A. Bohr and B. Mottelson, *Nuclear Structure* (Benjamin, Reading, Mass., 1975), Vol. 2.
[5] D. Bes, R. Broglia, and B. S. Nilsson, Phys. Rep. 16, 1 (1975).
[6] B. L. Berman and S. C. Fultz, Rev. Mod. Phys. 47, 713 (1975).
[7] R. A. Broglia, C. H. Dasso, and A. Winther, Phys. Lett. 51B, 113 (1976).
[8] J. Speth, in *Giant Multipole Resonances,* edited by F. E. Bertrand (Harwood Academic, New York, 1980), p. 33.
[9] R. Pitthan, in *Giant Multipole Resonances,* edited by F. E. Bertrand (Harwood Academic, New York, 1980), p. 161.
[10] R. A. Broglia, C. H. Dasso, H. Esbensen, A. Vitturi, and A. Winther, Nucl. Phys. A345, 263 (1980); R. A. Broglia, C. H. Dasso, H. Esbensen, and G. Pollarolo, Phys. Lett. 100B, 290 (1981).
[11] J. R. Nix and A. J. Sierk, Phys. Rev. C 25, 1068 (1982).
[12] M. Danos and W. Greiner, Phys. Rev. 138, B876 (1965).
[13] G. F. Bertsch, Phys. Lett. 37B, 470 (1971).
[14] C. B. Dover, R. H. Lemmer, and F. J. W. Hahne, Ann. Phys. (N.Y.) 70, 458 (1972).
[15] G. F. Bertsch, P. F. Bortignon, R. A. Broglia, and C. H. Dasso, Phys. Lett. 80B, 161 (1979).
[16] R. Broglia, in *Proceedings of the Nuclear Theory Summer Workshop, Santa Barbara, 1981,* edited by G. F. Bertsch (World Scientific, Singapore, 1982), p. 94.
[17] J. Wambash, V. K. Mishra, and Li Chu-Hsia, Nucl. Phys. A380, 285 (1982).
[18] N. Auerbach and A. Yeverechyan, Ann. Phys. (N.Y.) 95, 35 (1975).
[19] R. W. Hasse and P. Nerud, J. Phys. G 2, L101 (1976).
[20] G. Eckart, G. Holzwarth, and J. P. da Providencia, Nucl. Phys. A364, 1 (1981).
[21] H. Koch, G. Eckart, B. Schwesinger, and G. Holzwarth, Nucl. Phys. A373, 173 (1982).
[22] C. Y. Wong and N. Azziz, Phys. Rev. C 24, 2290 (1981); C. Y. Wong, *ibid.* 25, 2787 (1982).
[23] W. D. Meyers, W. J. Swiatecki, T. Kodama, L. J. El-Jaick, and E. R. Hilf, Phys. Rev. C 15, 203 (1977).
[24] R. A. Broglia and R. F. Bortignon, Phys. Lett. 101B, 135 (1981); P. F. Bortignon and R. A. Broglia, Nucl. Phys. A371, 405 (1981).
[25] L. G. Moretto and R. P. Schmitt, Rep. Prog. Phys. 44, 533 (1981).
[26] D. H. E. Gross, K. Möhring, S. Mukamel, U. Smilansky, and M. J. Sobel, Nucl. Phys. A378, 375 (1982); S. Mukamel, U. Smilansky, D. H. S. Gross, K. Möhring, and M. J. Sobel, *ibid.* A366, 339 (1981).
[27] N. Takigawa, K. Niita, Y. Okukara, and S. Yoshida, Nucl. Phys. A371, 130 (1981); K. Niita and N. Takigawa, *ibid.* 379, 141 (1983).
[28] S. Ayik and W. Nörenberg, Z. Phys. A 309, 121 (1982).
[29] J. P. Blaizot and Friman, Nucl. Phys. A373, 69 (1981).
[30] C. O. Dorso and E. S. Hernández, Phys. Rev. C 26, 528 (1982).
[31] C. George, J. Prigogine, and L. Rosenfeld, K. Dan. Vidensk. Selsk. Mat.-Fys. Medd. 38, 12 (1972).

[32]J. Prigogine, C. George, F. Henin, and L. Rosenfeld, Chem. Scr. 4, 5 (1972).
[33]R. Balescu, *Equilibrium and Nonequilibrium Statistical Mechanics* (Wiley Interscience, New York, 1975).
[34]F. Haake, in *Statistical Treatment of Open Systems by Generalized Master Equations,* Vol. 66 of *Springer Tracts in Modern Physics* (Springer, Berlin, 1973).
[35]S. Nakajima, Prog. Theor. Phys. 20, 948 (1958).
[36]R. W. Zwanzig, in *Lectures in Theoretical Physics,* edited by W. S. Brittin, B. W. Downs, and J. Downs (Interscience, New York, 1961).
[37]C. Dorso and E. S. Hernández, Nucl. Phys. A372, 215 (1981).
[38]E. S. Hernández and C. O. Dorso, Nucl. Phys. A399, 181 (1983).
[39]E. S. Hernández and C. O. Dorso, University of Buenos Aires Internal Report, 1982 (unpublished); C. O. Dorso, Ph.D. thesis, University of Buenos Aires, 1983 (unpublished).
[40]C. R. Willis and R. H. Picard, Phys. Rev. A 9, 1343 (1974).
[41]C. O. Dorso and E. S. Hernández, Phys. Rev. C (in press).
[42]E. S. Hernández and H. G. Solari, Nucl. Phys. A397, 115 (1983).
[43]U. Fano, Rev. Mod. Phys. 29, 74 (1957).
[44]R. W. Hasse, Rep. Prog. Phys. 41, 1027 (1978).
[45]H. Haken, *Synergetics* (Springer, Berlin, 1977).
[46]G. D. Smith, *Numerical Solution of Partial Differential Equations* (Oxford University Press, London, 1965).